BOUNDS ON $M_{H^\pm}$ FROM $\bar{B} \to X_{s,d}\gamma$ DECAYS*

Mikołaj Misiak

Institute of Theoretical Physics, Faculty of Physics, University of Warsaw
Pasteura 5, 02-093 Warszawa, Poland

(Received November 6, 2017)

Weak radiative B-meson decays are known to provide strong bounds on the charged Higgs boson mass in the Two-Higgs-Doublet Model. In the so-called Model-II, the 95% C.L. lower bound on $M_{H^\pm}$ is now in the 570–800 GeV range, depending quite sensitively on the method applied for its determination. Here, we present and discuss the updated bounds.

DOI:10.5506/APhysPolB.48.2173

One of the simplest extensions of the Standard Model (SM) is constructed by extending its Higgs sector via introduction of another $\mathrm{SU}(2)_{\mathrm{weak}}$ doublet. There are several versions of the Two-Higgs-Doublet Model (2HDM). In the so-called Model-I, fermions receive their masses from Yukawa couplings to only one of the two Higgs doublets. In Model-II, one of the doublets gives masses to the up-type quarks, while the other one gives masses to the down-type quarks and the leptons. The physical spin-zero boson spectrum contains a charged scalar $H^\pm$.

As it is well-known (see, *e.g.*, Ref. [1]), strong constraints on the mass of $H^\pm$ follow from measurements of the inclusive weak radiative B-meson decay branching ratio. The most precise results come from the Belle Collaboration, especially from their most recent analysis [2]. Their updated result is now below the Standard Model prediction [3, 4], though it remains consistent with it. On the other hand, the 2HDM effects in Model-II can only enhance the decay rate. In consequence, the lower bound on $M_{H^\pm}$ in this model becomes very strong, reaching the range of 570–800 GeV. At the same time, the bound becomes very sensitive to the method applied for its determination. Here, we present and discuss the current bounds, evaluated including the most recent experimental results and updated theoretical calculations. More details can be found in [5].

* Presented at the XLI International Conference of Theoretical Physics "Matter to the Deepest", Podlesice, Poland, September 3–8, 2017.

Following Eqs. (1.1) and (1.2) of Ref. [4], as well as Eq. (9) of Ref. [3], we use the CP- and isospin-averaged branching ratios $\mathcal{B}_{s\gamma}$ and $\mathcal{B}_{d\gamma}$ of the weak radiative decays, normalizing them to the analogously averaged branching ratio $\mathcal{B}_{c\ell\nu}$ of the semileptonic decay. The main observable for our considerations is the ratio $R_\gamma = (\mathcal{B}_{s\gamma} + \mathcal{B}_{d\gamma})/\mathcal{B}_{c\ell\nu} \equiv \mathcal{B}_{(s+d)\gamma}/\mathcal{B}_{c\ell\nu}$. The radiative decays we are interested in proceed dominantly via quark-level transitions $b \to s\gamma$, $b \to d\gamma$, and their C conjugates. A suppression by small Cabibbo–Kobayashi–Maskawa (CKM) angles makes $\mathcal{B}_{d\gamma}$ about 20 times smaller than $\mathcal{B}_{s\gamma}$. For definiteness, we shall discuss $\mathcal{B}_{s\gamma}$ in what follows, making separate comments on $\mathcal{B}_{d\gamma}$ wherever necessary.

Theoretical analyses of rare B-meson decays are most conveniently performed in the framework of an effective theory that arises after decoupling the W-boson and all the heavier particles at the renormalization scale $\mu_0 \sim m_t$. In the effective theory below μ_0, the relevant weak interaction Lagrangian takes the form of $\mathcal{L}_{\rm weak} \sim \sum_i C_i Q_i$, where Q_i are dimension-five and -six operators of either four-quark or dipole type. A complete list of Q_i that matter in the SM or 2HDM at the Leading Order (LO) in $\alpha_{\rm em}$ can be found in Eq. (1.6) of Ref. [4]. Their Wilson coefficients $C_i(\mu_0)$ are evaluated perturbatively in $\alpha_{\rm s}$ by matching several effective-theory Green's functions with those of the SM or 2HDM. Such calculations have now reached the Next-to-Next-to-Leading Order (NNLO) accuracy in QCD [6, 7]. In the next step, the Wilson coefficients are evolved according to their renormalization group equations down to the scale $\mu_b \sim m_b$, in order to resum large logarithms of the form of $\big(\alpha_{\rm s}\ln(\mu_0^2/\mu_b^2)\big)^n \sim \big(\alpha_{\rm s}\ln(m_t^2/m_b^2)\big)^n$. At the NNLO, anomalous dimension matrices up to four loops [8] had to be determined.

While the calculations of $C_i(\mu_b)$ are purely perturbative, one needs to take nonperturbative effects into account when determining the physical decay rates. For $\bar{B} \to X_s\gamma$ (with $\bar{B}$ denoting either $\bar{B}^0$ or B^-), the decay rate is a sum of the dominant perturbative contribution and a subdominant nonperturbative one $\delta\Gamma_{\rm nonp}$, *i.e.*

$$\Gamma\left(\bar{B} \to X_s\gamma\right) = \Gamma\left(b \to X_s^p\gamma\right) + \delta\Gamma_{\rm nonp}\,, \tag{1}$$

where a photon energy cutoff $E_\gamma > E_0$ in the decaying particle rest frame is imposed on both sides. The nonperturbative contribution $\delta\Gamma_{\rm nonp}$ in Eq. (1) is strongly dependent on E_0. For $E_0 = 1.6$ GeV, it shifts the SM prediction for $\mathcal{B}_{s\gamma}$ by almost $+3\%$ [9], while the corresponding uncertainty is estimated at the $\pm 5\%$ level [10]. For higher values of E_0, theoretical uncertainties grow, while the experimental ones decrease thanks to lower background subtraction errors. To resolve this issue, it has become standard to perform a data-driven extrapolation of the experimental results down to $E_0 = 1.6$ GeV, and compare with theory at that point.

A few comments about such an extrapolation need to be made. First, it is instructive to have a look at Fig. 1 of Ref. [2] which presents the background-subtracted photon energy (E_γ^*) spectrum in the $\Upsilon(4S)$ frame, as determined by Belle in Ref. [2]. Photon energies E_γ in the B-meson rest frame differ from E_γ^* by boost factors not exceeding 1.07. One can see that energies below 2 GeV are well in the tail of the spectrum. On the other hand, a large set of measurements that gives quite a precise weighted average for $\mathcal{B}_{(s+d)\gamma}$ is available already at $E_0 = 1.9$ GeV (see below). Thus, the extrapolation we need is a short one, and only in the tail of the spectrum.

To understand the growth of theoretical uncertainties with E_0, one begins with considering the case when C_7 is assumed to be the only nonvanishing Wilson coefficient at the scale μ_b. In such a case, the fixed-order Heavy Quark Effective Theory (HQET) formalism can be used to show that [11–13]

$$\left[\frac{\delta\Gamma_{\rm nonp}}{\Gamma\left(b \to X_s^p\gamma\right)}\right]_{\text{only } C_7} = -\frac{\mu_\pi^2 + 3\mu_G^2}{2m_b^2} + \mathcal{O}\left(\frac{\alpha_{\rm s}\Lambda^2}{(m_b - 2E_0)^2}, \frac{\Lambda^3}{m_b^3}\right), \qquad (2)$$

provided $m_b - 2E_0 \gg \Lambda$ with $\Lambda \sim \Lambda_{\rm QCD}$. The quantities μ_π^2 and μ_G^2 are of the order of Λ^2, and are currently quite well-known from fits to the measured semileptonic decay spectra [14]. With growing E_0, at some point one enters into the region, where $m_b - 2E_0 \sim \Lambda$ and the fixed-order HQET calculation is no longer applicable. Instead, the leading nonperturbative effect is parameterized in terms of a universal shape function [15, 16]. We need to rely on models for this function, which is the main reason why the theory uncertainties grow with E_0.

A number of shape-function models have been invented in the past, with their parameters constrained by measurements of the semileptonic and radiative B-meson decay spectra — see, *e.g.*, Refs. [17, 18]. In Fig. 13 of Ref. [18], one can see that the $\bar{B} \to X_s\gamma$ photon energy spectrum becomes quite unique already at $E_\gamma = 1.9$ GeV, at least for the considered class of models. Such a uniqueness is indeed expected below the point where the shape-function description starts to overlap with the fixed-order HQET description. Our present approach relies on the assumption that $E_0 = 1.6$ GeV is definitely below this point.

Effects of extrapolations from E_0 to 1.6 GeV can be parameterized by

$$\Delta_q \equiv \frac{\mathcal{B}_{q\gamma}(1.6)}{\mathcal{B}_{q\gamma}(E_0)} - 1\,, \qquad (3)$$

with $q = s, d$ or $s + d$. Numerical values of this quantity obtained with the help of various methods are presented in Table I. Those denoted by $\Delta_s^{\rm BF}$ were evaluated in Ref. [19] where the measured semileptonic and radiative

B-meson decay spectra were used to determine the b-quark mass m_b and the parameter μ_π^2 in three different renormalization schemes. Next, these parameters were inserted into the Kagan–Neubert shape function model [17]. The shape function was then convoluted with the perturbatively calculated photon energy spectrum in the b-quark decay, which led to a prediction for the physical photon energy spectrum in the B-meson decay.

TABLE I

Quantities Δ_q from Eq. (3) evaluated using various approaches.

E_0 [GeV]	$\Delta_s^{\rm BF}$	$\Delta_s^{\rm Belle}$	$\Delta_s^{\rm fix}$	$\Delta_{s+d}^{\rm fix}$	$\Delta_d^{\rm fix}$
1.7	$(1.5 \pm 0.4)\%$	?	1.3%	1.5%	5.3%
1.8	$(3.4 \pm 0.6)\%$	$(3.69 \pm 1.39)\%$	3.0%	3.4%	10.5%
1.9	$(6.8 \pm 1.1)\%$	?	5.5%	6.0%	15.7%
2.0	$(11.9 \pm 2.0)\%$	?	10.0%	10.5%	22.5%

In the next column of Table I, the quantities $\Delta_s^{\rm Belle}$ were obtained in Ref. [2] using essentially the same method but with the radiative spectrum only, as measured in the very analysis of Ref. [2]. In that case, only the result for $E_0 = 1.8$ GeV is publicly available at present.

The last three columns of Table I have been obtained using the approach of Refs. [3, 4], in which case the photon energy spectrum is determined mainly by the perturbative gluon bremsstrahlung. In these cases, no uncertainties are quoted, as we do not know at which E_0 the fixed-order HQET description breaks down. The subleading $\mathcal{O}(\alpha_{\rm s}\Lambda^2)$ nonperturbative corrections [20] begin to rapidly increase at E_0 around 1.8 GeV due to $(m_b - 2E_0)^2$ in their denominators. The quantities $\Delta_q^{\rm fix}$ involve effects of the photon bremsstrahlung in decays of the b quark to three light (anti)quarks, as calculated in Refs. [21, 22]. Such effects are small in $\mathcal{B}_{s\gamma}$ (unless one goes well below $E_0 = 1.6$ GeV) but become much more relevant in $\mathcal{B}_{d\gamma}$, where the tree-level $b \to du\bar{u}\gamma$ transitions are not CKM-suppressed with respect to the leading $b \to d\gamma$ one. In effect, $\Delta_d^{\rm fix}$ are visibly different from $\Delta_s^{\rm fix}$. However, $\Delta_{s+d}^{\rm fix}$ is not much different from $\Delta_s^{\rm fix}$ due to the dominance of $\mathcal{B}_{s\gamma}$ over $\mathcal{B}_{d\gamma}$. Such photon bremsstrahlung effects involve collinear singularities in the limit of vanishing quark masses, which signals the presence of nonperturbative effects [23]. Fortunately, their overall suppression factors in $\mathcal{B}_{s\gamma}$ and $\mathcal{B}_{(s+d)\gamma}$ are strong enough, and the corresponding uncertainties are far below the dominant nonperturbative ones. In the following, we shall use $\Delta_s^{\rm BF}$ for the extrapolation of $\mathcal{B}_{s\gamma}$. As far as the extrapolation of $\mathcal{B}_{(s+d)\gamma}$ is concerned, we are going to rescale $\Delta_s^{\rm BF}$ according to the fixed-order results, namely use $\Delta_{s+d}^{\rm BF} \equiv \Delta_s^{\rm BF} \times \Delta_{s+d}^{\rm fix}/\Delta_s^{\rm fix}$.

For the evaluation of $\Gamma(b \to X_s^p\gamma)$ at the NNLO level, we can restrict our attention to the current–current operators $Q_{1,2}$ and the dipole ones $Q_{7,8}$, as the remaining ones can be neglected due to their small Wilson coefficients. The Q_7–Q_7 and Q_7–Q_8 interference terms are already known at $\mathcal{O}(\alpha_s^2)$ in a complete manner [24–28]. The NNLO interference terms not involving Q_7 can be separated into known two-body final-state contributions or relatively small ($n \geq 3$)-body final-state contributions that have been calculated so far [29–31] only in the Brodsky–Lepage–Mackenzie (BLM) [32] approximation. The main perturbative uncertainty comes from the $Q_{1,2}$–Q_7 interferences at $\mathcal{O}(\alpha_s^2)$. Their BLM parts, as well as effects of nonvanishing quark masses on the gluon lines were evaluated in Refs. [29, 33, 34] for arbitrary values of the charm quark mass m_c. The remaining parts were found only in the limits $m_c \gg m_b/2$ [35] or $m_c = 0$ [4], and then an interpolation between these two limits was performed [4].

With all the NNLO QCD, NLO EW and nonperturbative corrections evaluated to date, the SM prediction for R_γ at $E_0 = 1.6$ GeV reads [3]

$$R_\gamma^{\mathrm{SM}} = (3.31 \pm 0.22) \times 10^{-3}\,, \tag{4}$$

where the overall uncertainty has been obtained by combining in quadrature the nonperturbative one ($\pm 5\%$), the parametric one ($\pm 1.5\%$), the one stemming from neglected higher order effects ($\pm 3\%$), and the one due to the above-mentioned interpolation in m_c ($\pm 3\%$).

In the 2HDM, additional contributions to the Wilson coefficient matching arise from diagrams with the physical charged scalar exchanges. The relevant couplings and sample diagrams can be found, *e.g.*, in Sec. 2.3 of Ref. [7]. Apart from the SM parameters, the results depend only on $M_{H^\pm}$ and $\tan\beta$. They are plotted in Fig. 1 as functions of $M_{H^\pm}$ in two cases of particular interest: Model-I with $\tan\beta = 1$ and Model-II with $\tan\beta = 50$. The solid and dashed curves in these plots correspond to the 2HDM and SM cases, respectively. Dotted lines indicate the experimental average to be discussed below.

In Model-I, the charged Higgs contribution to the decay amplitude is proportional to $\cot^2\beta$, and it interferes with the SM one in a destructive manner. In Model-II, the interference is always constructive, and the charged Higgs amplitude has the form of $A + B\cot^2\beta$. The quantities A and B depend on $M_{H^\pm}$ only, and they have the same sign. In consequence, an absolute bound on $M_{H^\pm}$ can be derived from R_γ in Model-II by setting the $\cot^2\beta$ term to zero.

Our averages of all the available measurements of $\mathcal{B}_{(s+d)\gamma}$ and $\mathcal{B}_{s\gamma}$ are collected in Table II. The results of BaBar have been obtained using three methods: fully inclusive [36], semi-inclusive [37], and the hadronic-tag one [38]. Belle has used the fully inclusive [2] and semi-inclusive [39] approaches. In

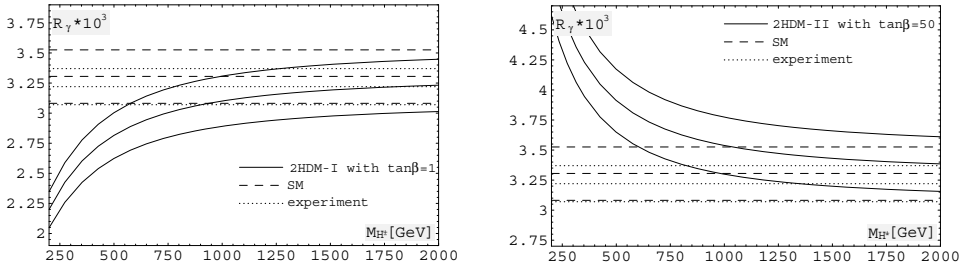

Fig. 1. R_γ at $E_0 = 1.6$ GeV as a function of $M_{H^\pm}$ in Model-I with $\tan\beta = 1$ (left) and in Model-II with $\tan\beta = 50$ (right). Middle lines show the central values, while the upper and lower ones are shifted by $\pm 1\sigma$. Solid and dashed curves correspond to the 2HDM and SM predictions, respectively. Dotted lines show the experimental average $R_\gamma^{\rm exp} = (3.22 \pm 0.15) \times 10^{-3}$ (see the text).

the measurement of CLEO [40], the fully inclusive method was used. Belle and CLEO provided their $\mathcal{B}_{(s+d)\gamma}$ results explicitly, while BaBar rescaled them to $\mathcal{B}_{s\gamma}$, quoting in each case the necessary CKM factor together with its uncertainty. In Table II, we "undo" the rescaling using precisely the same factors. On the other hand, in the two semi-inclusive cases, we derive $\mathcal{B}_{(s+d)\gamma}$ from $\mathcal{B}_{s\gamma}$ using a rescaling factor (1.047 ± 0.003) that we calculate at $E_0 = 1.9$ GeV as in Refs. [3, 4].

TABLE II

Averages of the experimental results for $\mathcal{B}_{s\gamma} \times 10^6$ (upper rows) and $\mathcal{B}_{(s+d)\gamma} \times 10^6$ (lower rows) at each value of E_0. Each world average (w.a.) is first calculated at E_0 ($5^{\rm th}$ column), and then extrapolated to 1.6 GeV ($6^{\rm th}$ column) using $\Delta_s^{\rm BF}$ or $\Delta_{s+d}^{\rm BF}$ (see Table I). In the last two columns, the ratios $R_\gamma(\times 10^5)$ are calculated from the corresponding averages for $\mathcal{B}_{(s+d)\gamma}$ using $\mathcal{B}_{c\ell\nu} = 0.1067(16)$.

E_0	BaBar [36–38]	Belle [2, 39]	CLEO [40]	w.a. (E_0)	w.a. (1.6)	R_γ (E_0)	R_γ (1.6)
1.7		306(28)		306(28)	311(28)		
		320(29)		320(29)	326(30)	300(28)	305(28)
1.8	321(34)	301(22)		307(19)	318(19)		
	335(35)	315(23)		321(19)	333(20)	301(19)	312(19)
1.9	308(22)	305(16)		306(13)	327(14)		
	321(23)	319(17)		320(14)	343(15)	300(14)	322(15)
2.0	283(18)	279(15)	293(46)	281(11)	315(14)		
	296(19)	292(15)	306(49)	294(11)	331(14)	276(11)	310(14)

The reader is referred to the original experimental papers [2, 36–40] for the decomposition of errors into the statistical, systematic and occasionally the spectrum-modeling ones. Here, we have added them in quadrature for the purpose of determining our naive averages, in which no correlations have been taken into account. At $E_0 = 1.9$ GeV (without extrapolation), we find agreement with the averages of HFLAV [41] where, we believe, the relevant correlations have been included.

Comparing the uncertainties in the four alternative averages for R_γ at $E_0 = 1.6$ GeV in the last column of Table II, one can see that the first two of them are less accurate. Thus, at the moment, the balance of the background subtraction and extrapolation uncertainties points towards using the results extrapolated from 1.9 or 2.0, at least when one takes the errors from Ref. [19] for granted. Since there is not much difference in the uncertainties of these two averages, we suggest discarding the 2.0 one, as it requires a longer extrapolation. Thus, we recommend adopting

$$R_\gamma^{\rm exp} = (3.22 \pm 0.15) \times 10^{-3} \tag{5}$$

as the current experimental average for R_γ at $E_0 = 1.6$ GeV.

Let us now use R_γ to derive bounds on $M_{H^\pm}$ in the 2HDM. We are going to treat all the uncertainties as stemming from Gaussian probability distributions, which is obviously an *ad hoc* assumption, although consistent with combining various partial uncertainties in quadrature. To include the theory uncertainties, one follows the standard confidence belt construction [42]. For each $M_{H^\pm}$, one considers a Gaussian probability distribution around the theoretical central value, with its variance obtained by combining the experimental and theoretical uncertainties in quadrature. Next, a confidence interval corresponding to (say) 95% integrated probability is determined. It can be placed either centrally (for a derivation of 2-sided bounds), or maximally shifted in either way (for 1-sided bounds), or in an intermediate way, like in the Feldman–Cousins (FC) approach [43]. It is the freedom of the confidence interval placement that makes the resulting bounds on $M_{H^\pm}$ somewhat ambiguous. If we choose the FC intervals, low values of $R_\gamma^{\rm exp}$ can never lead to exclusion of Model-II in its whole parameter space. If we choose the upper 1-sided intervals, our method is actually equivalent to using the experimental upper bound on $R_\gamma^{\rm exp}$ rather than the actual measurement.

In Table III, we present the bounds we obtain following three different methods, and using three out of four averages for $R_\gamma^{\rm exp}$ from Table II. The rows corresponding to our preferred choice (Eq. (5)) are displayed in bold. For Model-I we set $\tan\beta = 1$, while the absolute bounds ($\cot\beta \to 0$) are shown for Model-II. In the Model-I case, the lower rather than the upper 1-sided intervals are employed. It is interesting to observe that stronger

TABLE III

Bounds on $M_{H^\pm}$ obtained using different methods (see the text).

Model	$R_\gamma^{\rm exp} \times 10^3$	95% C.L. bounds			99% C.L. bounds		
		1-s	2-s	FC	1-s	2-s	FC
	3.05 ± 0.28	307	268	268	230	208	208
I	3.12 ± 0.19	401	356	356	313	288	288
($\tan\beta = 1$)	$\mathbf{3.22 \pm 0.15}$	**504**	**445**	**445**	**391**	**361**	**361**
	3.05 ± 0.28	740	591	569	477	420	411
II	3.12 ± 0.19	795	645	628	528	468	461
(absolute)	$\mathbf{3.22 \pm 0.15}$	**692**	**583**	**580**	**490**	**440**	**439**

bounds on $M_{H^\pm}$ in Model-II are found from the two less precise averages, just because their central values turn out to be lower. These averages are less sensitive to the E_0-extrapolation issues. The situation in Model-I is reverse — the most precise average gives the strongest bounds. By coincidence, our 2-sided 95% C.L. bound of 583 GeV in Model-II practically overlaps with the 580 GeV one that has been obtained in Ref. [2] from their single measurement alone (giving $\mathcal{B}_{(s+d)\gamma}$ with a lower central value but larger uncertainty than the one corresponding to our Eq. (5)). Since this bound is also the most conservative one, we suggest choosing it for updated combinations with constraints from other observables.

To conclude, we derived updated constraints on $M_{H^\pm}$ in the 2HDM that get imposed by measurements of the inclusive weak radiative B-meson decay branching ratio.

Partial support from the National Science Centre, Poland (NCN) research project, decision No. DEC-2014/13/B/ST2/03969 is gratefully acknowledged.

REFERENCES

[1] A.J. Buras, M. Misiak, M. Münz, S. Pokorski, *Nucl. Phys. B* **424**, 374 (1994).
[2] A. Abdesselam *et al.* [Belle Collaboration], `arXiv:1608.02344 [hep-ex]`.
[3] M. Misiak *et al.*, *Phys. Rev. Lett.* **114**, 221801 (2015).
[4] M. Czakon *et al.*, *J. High Energy Phys.* **1504**, 168 (2015).
[5] M. Misiak, M. Steinhauser, *Eur. Phys. J. C* **77**, 201 (2017).
[6] M. Misiak, M. Steinhauser, *Nucl. Phys. B* **683**, 277 (2004).

[7] T. Hermann, M. Misiak, M. Steinhauser, *J. High Energy Phys.* **1211**, 036 (2012).
[8] M. Czakon, U. Haisch, M. Misiak, *J. High Energy Phys.* **0703**, 008 (2007).
[9] G. Buchalla, G. Isidori, S.J. Rey, *Nucl. Phys. B* **511**, 594 (1998).
[10] M. Benzke, S.J. Lee, M. Neubert, G. Paz, *J. High Energy Phys.* **1008**, 099 (2010).
[11] I.I.Y. Bigi, N.G. Uraltsev, A.I. Vainshtein, *Phys. Lett. B* **293**, 430 (1992) [*Erratum ibid.* **297**, 477 (1992)].
[12] I.I.Y. Bigi *et al.*, `arXiv:hep-ph/9212227`.
[13] A.F. Falk, M. Luke, M.J. Savage, *Phys. Rev. D* **49**, 3367 (1994).
[14] A. Alberti, P. Gambino, K.J. Healey, S. Nandi, *Phys. Rev. Lett.* **114**, 061802 (2015).
[15] M. Neubert, *Phys. Rev. D* **49**, 4623 (1994).
[16] I.I.Y. Bigi *et al.*, *Int. J. Mod. Phys. A* **9**, 2467 (1994).
[17] A.L. Kagan, M. Neubert, *Eur. Phys. J. C* **7**, 5 (1999).
[18] Z. Ligeti, I.W. Stewart, F.J. Tackmann, *Phys. Rev. D* **78**, 114014 (2008).
[19] O. Buchmüller, H. Flächer, *Phys. Rev. D* **73**, 073008 (2006).
[20] T. Ewerth, P. Gambino, S. Nandi, *Nucl. Phys. B* **830**, 278 (2010).
[21] M. Kamiński, M. Misiak, M. Poradziński, *Phys. Rev. D* **86**, 094004 (2012).
[22] T. Huber, M. Poradziński, J. Virto, *J. High Energy Phys.* **1501**, 115 (2015).
[23] H.M. Asatrian, C. Greub, *Phys. Rev. D* **88**, 074014 (2013).
[24] I.R. Blokland *et al.*, *Phys. Rev. D* **72**, 033014 (2005).
[25] K. Melnikov, A. Mitov, *Phys. Lett. B* **620**, 69 (2005).
[26] H.M. Asatrian, T. Ewerth, H. Gabrielyan, C. Greub, *Phys. Lett. B* **647**, 173 (2007).
[27] T. Ewerth, *Phys. Lett. B* **669**, 167 (2008).
[28] H.M. Asatrian *et al.*, *Phys. Rev. D* **82**, 074006 (2010).
[29] Z. Ligeti, M.E. Luke, A.V. Manohar, M.B. Wise, *Phys. Rev. D* **60**, 034019 (1999).
[30] A. Ferroglia, U. Haisch, *Phys. Rev. D* **82**, 094012 (2010).
[31] M. Misiak, M. Poradziński, *Phys. Rev. D* **83**, 014024 (2011).
[32] S.J. Brodsky, G.P. Lepage, P.B. Mackenzie, *Phys. Rev. D* **28**, 228 (1983).
[33] K. Bieri, C. Greub, M. Steinhauser, *Phys. Rev. D* **67**, 114019 (2003).
[34] R. Boughezal, M. Czakon, T. Schutzmeier, *J. High Energy Phys.* **0709**, 072 (2007).
[35] M. Misiak, M. Steinhauser, *Nucl. Phys. B* **840**, 271 (2010).
[36] J.P. Lees *et al.* [BaBar Collaboration], *Phys. Rev. Lett.* **109**, 191801 (2012).
[37] J.P. Lees *et al.* [BaBar Collaboration], *Phys. Rev. D* **86**, 052012 (2012).
[38] B. Aubert *et al.* [BaBar Collaboration], *Phys. Rev. D* **77**, 051103 (2008).

[39] T. Saito *et al.* [Belle Collaboration], *Phys. Rev. D* **91**, 052004 (2015).

[40] S. Chen *et al.* [CLEO Collaboration], *Phys. Rev. Lett.* **87**, 251807 (2001).

[41] Y. Amhis *et al.* [Heavy Flavor Averaging Group], `arXiv:1612.07233 [hep-ex]`.

[42] C. Patrignani *et al.* [Particle Data Group], *Chin. Phys. C* **40**, 100001 (2016).

[43] G.J. Feldman, R.D. Cousins, *Phys. Rev. D* **57**, 3873 (1998).